

LHC SUSY and WIMP dark matter searches confront the string theory landscape

Howard Baer^{1*}, Vernon Barger^{2†}, Shadman Salam^{1‡},
Hasan Serce^{2§} and Kuver Sinha^{1¶}

¹*Dept. of Physics and Astronomy, University of Oklahoma, Norman, OK 73019, USA*

²*Dept. of Physics, University of Wisconsin, Madison, WI 53706 USA*

Abstract

The string theory landscape of vacua solutions provides physicists with some understanding as to the magnitude of the cosmological constant. Similar reasoning can be applied to the magnitude of the soft SUSY breaking terms in supersymmetric models of particle physics: there appears to be a statistical draw towards large soft terms which is tempered by the anthropic requirement of the weak scale lying not too far from ~ 100 GeV. For a mild statistical draw of m_{soft}^n with $n = 1$ (as expected from SUSY breaking due to a single F term) then the light Higgs mass is preferred at ~ 125 GeV while sparticles are all pulled beyond LHC bounds. We confront a variety of LHC and WIMP dark matter search limits with the statistical expectations from a fertile patch of string theory landscape. The end result is that LHC and WIMP dark matter detectors see exactly that which is expected from the landscape: a Standard Model-like Higgs boson of mass 125 GeV but as yet no sign of sparticles or WIMP dark matter. SUSY from the $n = 1$ landscape is most likely to emerge at LHC in the soft opposite-sign dilepton plus jet plus MET channel. Multi-ton noble liquid WIMP detectors should be able to completely explore the $n = 1$ landscape parameter space.

*Email: baer@ou.edu

†Email: barger@pheno.wisc.edu

‡Email: shadman.salam@ou.edu

§Email: serce@ou.edu

¶Email: kuver.sinha@ou.edu

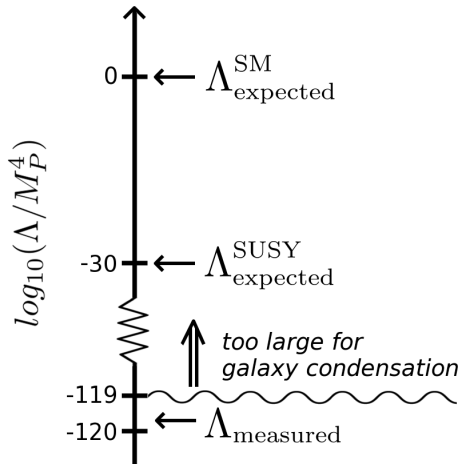


Figure 1: Log portrayal of expected parameter space of the cosmological constant Λ from the string theory landscape.

1 Introduction

It is sometimes lamented that the emergence of the landscape of string vacua [1–3] has rendered string theory non-predictive since how are we to pick out the (meta-stable) vacuum corresponding to our universe from (perhaps) of order 10^{500} possibilities? Such sentiment ignores one of the great predictions of the latter 20th century [4]: namely that given a multiverse which includes a vast assortment of pocket-universes with varying cosmological constants, then it may not be surprising to find $\Lambda \sim 10^{-120} m_P^4$ since if it was much bigger, then galaxy condensation would not occur and we would not even be here to discuss the issue. The situation is portrayed in Fig. 1 which depicts the fact that the cosmological constant ought to be at its most natural value *subject to the constraint that we can exist to observe it*. Such anthropic reasoning relies on the existence of a vast landscape of possibilities that is provided for by the discretuum of flux vacua from string theory [1–3, 5].

Can such reasoning be applied to the origin of other mass scales that appear in fundamental physics?¹ An obvious target would be the magnitude of the weak scale ($m_{weak} \simeq m_{W,Z,h} \simeq 100$ GeV) and why it is suppressed by 16 orders of magnitude compared to the (reduced) Planck scale $m_P \simeq 2.4 \times 10^{18}$ GeV. Anthropically, one expects a universe with electroweak symmetry properly broken such that weak bosons gain mass $m_{W,Z} \sim 100$ GeV while solutions with charge or color breaking minima would be excluded. In addition, nuclear physics calculations by Agrawal *et al.* [7] require that the magnitude of the weak scale shouldn't exceed its measured value by a factor of 2-3 in order to gain a livable universe.

Given that quantum corrections to the Higgs mass diverge quadratically with the theory cutoff Λ_{SM} , it seems the Standard Model (SM) with $\Lambda_{SM} \gg m_{weak}$ would be a rare occurrence

¹Weinberg states [6]: “The most optimistic hypothesis is that the only constants that scan are the few whose dimensionality is a positive power of mass: the vacuum energy, and whatever scalar mass or masses set the scale of electroweak symmetry breaking.”

within the landscape since one would be required to select only those vacuum solutions with highly fine-tuned scan parameters. In a landscape containing both SM and supersymmetric SM solutions (SSM), one would expect vastly more SSM solutions with $m_{weak} \simeq 100$ GeV since then quantum corrections to m_h diverge only logarithmically.

In fact, this discussion brings up the issue of how naturalness is connected to vacua selection in the multiverse. Here we adopt the notion of *practical naturalness*:

An observable $\mathcal{O} \equiv o_1 + \dots + o_n$ is natural if all *independent* contributions o_i to \mathcal{O} are comparable to or less than \mathcal{O} .

This is because if any $o_i \gg \mathcal{O}$, then some other contribution o_j ($j \neq i$) would have to be fine-tuned to a large opposite-sign value to keep \mathcal{O} at its measured value. The notion of practical naturalness may be compared with what Douglas calls stringy naturalness [8]:

An effective field theory (or specific coupling or observable) T_1 is more natural in string theory than T_2 if the number of *phenomenologically acceptable* vacua leading to T_1 is larger than the number leading to T_2 .

In a landscape of vacua where independent contributions o_i to observable \mathcal{O} are uniformly distributed, then it follows that many more vacua are likely to exist where the o_i are comparable to \mathcal{O} than where some $o_i \gg \mathcal{O}$ so that some other value $o_{j \neq i} \simeq -o_i$. Thus, we expect these two definitions to be equivalent descriptions of naturalness. The landscape, if it is to be predictive, is predictive in the statistical sense: the more prevalent solutions are statistically more likely. This gives the connection between landscape statistics and naturalness: vacua with natural observables are expected to be far more common than vacua with unnatural observables.²

Thus, in this paper we will focus on vacua solutions which include the Minimal Supersymmetric Standard Model (MSSM) as their weak scale effective theory. This restricts our attention to a *fertile patch* of landscape solutions which include the SM as the weak scale effective theory (in accord with experiment) but where the weak scale is stable against quantum corrections (as in the MSSM). We will further assume that the MSSM arises from a 4-d supergravity theory (SUGRA) where SUSY breaking occurs via spontaneous SUGRA breaking in a hidden sector of the theory with a, perhaps, complicated SUSY breaking sector including possibly numerous SUSY breaking F - and D -term fields which gain vevs. The question that can be addressed is then: what does a statistical sampling of this fertile patch of the landscape say about the scale of SUSY breaking, and hence the likelihood of observable signals at the CERN Large Hadron Collider (LHC) or at WIMP dark matter direct and indirect detection experiments? Indeed, this question has already been investigated early on by Douglas *et al.* [10–12], Susskind [9] and by Dine *et al.* [13]. (For some reviews, see *e.g.* Ref's [14, 15].)

²Since the landscape allows for an apparently unnatural value of $\Lambda_{cc} \ll m_P^4$, it is sometimes interpreted that vacua with *other* highly unnatural observables should also be entertained. In the case of Λ_{cc} , we should find ourselves in a universe where the cosmological constant is *as natural as possible* such that we gain a livable universe. Then we would expect $\Lambda_{cc} \sim 10^{-120} m_P^4$ rather than say $10^{-200} m_P^4$.

2 Statistics of the SUSY breaking scale

In this Section, we assume a vast ensemble of string vacua states which give rise to a $D = 4$, $N = 1$ supergravity effective field theory at high energies. Furthermore, the theory consists of a visible sector containing the MSSM along with a perhaps large assortment of fields that comprise the hidden sector. The scalar potential is given by the usual supergravity form [16]

$$V = e^{K/m_P^2} \left(g^{i\bar{j}} D_i W D_{\bar{j}} W^* - \frac{3}{m_P^2} |W|^2 \right) + \frac{1}{2} \sum_{\alpha} D_{\alpha}^2 \quad (1)$$

$$= e^{K/m_P^2} \left(\sum_i |F_i|^2 - 3 \frac{|W|^2}{m_P^2} \right) + \frac{1}{2} \sum_{\alpha} D_{\alpha}^2 \quad (2)$$

where W is the holomorphic superpotential, K is the real Kähler potential and $F_i = D_i W = DW/D\phi^i \equiv \partial W/\partial\phi^i + (1/m_P^2)(\partial K/\partial\phi^i)W$ are the F -terms and $D_{\alpha} \sim \sum \phi^{\dagger} g_{\alpha} \phi$ are the D -terms and the ϕ^i are chiral superfields. Supergravity is assumed to be broken spontaneously via the super-Higgs mechanism either via F -type breaking or D -type breaking or in general a combination of both leading to a gravitino mass $m_{3/2} = e^{K/2m_P^2} |W|/m_P^2$. The (metastable) minima of the scalar potential can be found by requiring $\partial V/\partial\phi^i = 0$ with $\partial^2 V/\partial\phi^i \partial\phi^j > 0$ to ensure a local minimum. The cosmological constant is given by

$$\Lambda_{cc} = m_{hidden}^4 - 3e^{K/m_P^2} |W|^2/m_P^2 \quad (3)$$

where $m_{hidden}^4 = \sum_i |F_i|^2 + \frac{1}{2} \sum_{\alpha} D_{\alpha}^2$ is a mass scale associated with the hidden sector (and usually in SUGRA-mediated models it is assumed $m_{hidden} \sim 10^{12}$ GeV such that the gravitino gets a mass $m_{3/2} \sim m_{hidden}^2/m_P$).

According to Douglas *et al.* [11] from investigations of flux compactifications in IIB string theory, the distribution of vacua ought to have the form

$$dN_{vac}[m_{hidden}^2, m_{weak}, \Lambda] = f_{SUSY}(m_{hidden}^2) \cdot f_{EWFT} \cdot f_{cc} \cdot dm_{hidden}^2 \quad (4)$$

where we define the weak scale $m_{weak} \simeq m_{W,Z,h} \simeq 100$ GeV and where m_{hidden} sets the scale for SUSY breaking with $m_{hidden}^2 = \sum_i |F_i|^2 + \frac{1}{2} \sum_{\alpha} D_{\alpha}^2$ for a (in general) more complicated SUSY breaking sector containing multiple sources of SUSY breaking, as may be expected to occur in string theory.

The function f_{SUSY} contains the expected statistical distribution of SUSY breaking scales. This is related to the mass scale of MSSM soft terms as $m_{soft} \simeq m_{hidden}^2/m_P$. If the sources of SUSY breaking have uniformly distributed vacuum expectation values (vevs), then it is surmised that

$$f_{SUSY}(m_{hidden}^2) \sim (m_{hidden}^2)^{2n_F+n_D-1} \quad (5)$$

where n_F is the number of F -breaking fields and n_D is the number of D -term breaking fields in the hidden sector [8–11]. We will denote the collective exponent in f_{SUSY} as $n \equiv 2n_F + n_D - 1$. Since the F terms are complex-valued but the modulus $|F|$ sets the scale of SUSY breaking, then they contribute as $(m_{hidden}^2)^{2n_F}$ whereas the real valued D terms contribute as $(m_{hidden}^2)^{n_D}$. In terms of MSSM soft SUSY breaking parameters, one would expect a statistically *uniform*

distribution of soft terms m_{soft}^0 only for a single D -term breaking field so that $n_D = 1$. A single F -term breaking field leads to $f_{SUSY} \sim m_{soft}^1$ so that there is a linearly increasing preference for large soft terms. For more complex configurations with larger number of n_F and n_D , then there is an even greater statistical preference for large soft terms which could lead to a preference for models with high scale SUSY breaking.

Regarding the role of the cosmological constant in determining the SUSY breaking scale, a key observation of Denef and Douglas [10, 11] and Susskind [9] was that W at the minima is distributed uniformly as a complex variable, and the distribution of $e^{K/m_P^2}|W|^2/m_P^2$ is not correlated with the distributions of F_i and D_α . Setting the cosmological constant to nearly zero, then, has no effect on the distribution of supersymmetry breaking scales. Physically, this can be understood by the fact that the superpotential receives contributions from many sectors of the theory, supersymmetric as well as non-supersymmetric. The cosmological fine-tuning penalty is $f_{cc} \sim \Lambda/m^4$ where the above discussion leads to $m^4 \sim m_{string}^4$ rather than $m^4 \sim m_{hidden}^4$, rendering this term inconsequential for determining the number of vacua with a given SUSY breaking scale.

The final term f_{EWFT} merits some discussion. Following Ref. [17], an initial guess [9, 11, 13] for f_{EWFT} was that $f_{EWFT} \sim m_{weak}^2/m_{soft}^2$ which may be interpreted as conventional naturalness in that the larger the Little Hierarchy between m_{weak} and m_{soft} , then the greater is the fine-tuning penalty. As pointed out in Ref. [18], there are several problems with this ansatz.

1. As soft terms such as the trilinear A_t terms increase, one is ultimately forced into charge-color-breaking vacua of the MSSM [19, 20]. These sorts of vacua must be entirely vetoed on anthropic grounds.
2. As high-scale soft terms such as $m_{H_u}^2$ increase too much, then they are no longer driven to negative values and electroweak symmetry isn't even broken. These non-EWSB solutions also should be vetoed on anthropic grounds.
3. As the high scale soft term $m_{H_u}^2$ increases, its weak scale value actually becomes smaller and smaller until EWSB is barely broken [21, 22]. This means the *weak scale* value of $m_{H_u}^2$ becomes more natural— a phenomena known as *radiatively driven naturalness* (RNS) [23, 24].
4. As the soft term A_t increases, then cancellations can occur in the $\Sigma_u^u(\tilde{t}_{1,2})$ contributions to the weak scale scalar potential, rendering their contributions closer to, not further from, the weak scale whilst at the same time lifting up the Higgs mass m_h to the 125 GeV range.
5. Even in the event of appropriate EWSB, the factor $f_{EWFT} \sim m_{weak}^2/m_{soft}^2$ penalizes but does not forbid vacua with a weak scale far larger than its measured value. In contrast, Agrawal *et al.* [7] have shown that a weak scale larger than ~ 3 times its measured value would lead to much weaker weak interactions and a disruption in nuclear synthesis reactions, and likely an unlivable universe as we know it. In addition, Susskind posits that an increased weak scale would lead to larger SM particle masses and consequent disruptions in both atomic and nuclear physics. From these calculations, it seems reasonable to

veto SM-like vacua which lead to a weak scale more than (conservatively) four times its measured value.

To account for these issues, in Ref. [18] the alternative of

$$f_{EWFT} \sim \Theta(30 - \Delta_{EW}) \quad (6)$$

was suggested where Δ_{EW} is the electroweak fine-tuning measure which just requires that *weak scale* contributions to m_Z^2 should be comparable to or less than m_Z^2 . From the minimization conditions for the MSSM Higgs potential [25] one finds

$$\frac{m_Z^2}{2} = \frac{m_{H_d}^2 + \Sigma_d^d - (m_{H_u}^2 + \Sigma_u^u) \tan^2 \beta}{\tan^2 \beta - 1} - \mu^2 \simeq -m_{H_u}^2 - \Sigma_u^u - \mu^2. \quad (7)$$

The naturalness measure Δ_{EW} compares the largest contribution on the right-hand-side of Eq. 7 to the value of $m_Z^2/2$. The radiative corrections Σ_u^u and Σ_d^d include contributions from various particles and sparticles with sizeable Yukawa and/or gauge couplings to the Higgs sector. Usually the most important of these are

$$\Sigma_u^u(\tilde{t}_{1,2}) = \frac{3}{16\pi^2} F(m_{\tilde{t}_{1,2}}^2) \left[f_t^2 - g_Z^2 \mp \frac{f_t^2 A_t^2 - 8g_Z^2(\frac{1}{4} - \frac{2}{3}x_W)\Delta_t}{m_{\tilde{t}_2}^2 - m_{\tilde{t}_1}^2} \right] \quad (8)$$

where f_t is the top-quark Yukawa coupling, $\Delta_t = (m_{\tilde{t}_L}^2 - m_{\tilde{t}_R}^2)/2 + M_Z^2 \cos 2\beta(\frac{1}{4} - \frac{2}{3}x_W)$, $x_W \equiv \sin^2 \theta_W$, $F(m^2) = m^2 \left(\log \frac{m^2}{Q^2} - 1 \right)$ and the optimized scale choice for evaluation of these corrections is $Q^2 = m_{\tilde{t}_1} m_{\tilde{t}_2}$. In the denominator of Eq. 8, the tree level expressions of $m_{\tilde{t}_{1,2}}^2$ should be used. Expressions for the remaining Σ_u^u and Σ_d^d terms are given in the Appendix of Ref. [24].

In the remainder of this paper, we will assume a solution to the SUSY μ problem such as the gravity-safe, electroweak natural axionic hybrid CCK model based on a \mathbb{Z}_{24}^R symmetry in Ref. [26]. As such, we invert the usual usage of Δ_{EW} with fluid soft terms and μ term: instead, the weak scale (as typified by the value of m_Z) is no longer fixed at its measured value but is instead *determined* by Eq. 7. In this case, values of $\Delta_{EW} \gtrsim 30$ correspond to a value of $m_{weak} \gtrsim$ four times its measured value (in our sub-universe). The Θ function in Eq. 6 guarantees that we veto vacua with CCB minima or no EWSB. It also vetoes properly broken Higgs potentials but where the weak scale is generated at more than four times its measured value.

2.1 Brief review of some previous work and goals of the present work

In Ref. [22], an approach similar to Weinberg's anthropic solution to the cosmological constant was applied to determination of the SUSY breaking scale. It was assumed that there was a mild draw of the landscape towards large soft terms which was tempered by the anthropic requirement of a value for the weak scale which was not too far from its measured value by a factor \sim four. The draw of $m_{H_u}^2$ towards large values, tempered by an appropriate breakdown of

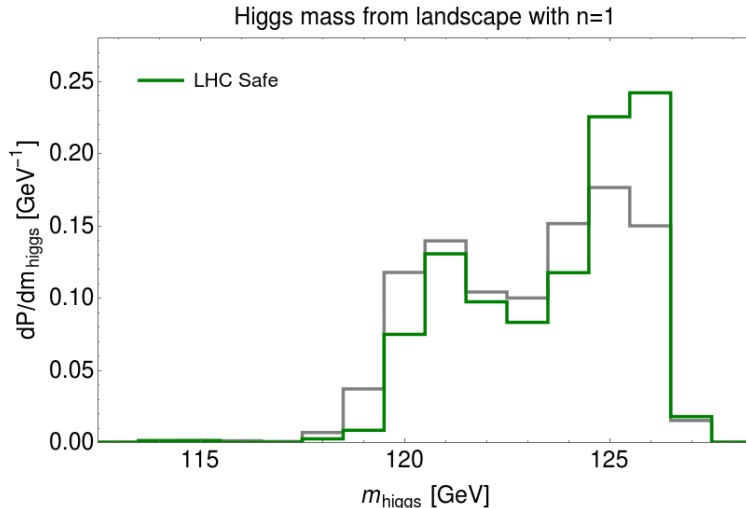


Figure 2: Statistical expectation for the mass of the Higgs boson from the string theory landscape which scans over single F -term SUSY breaking. The green histogram includes only LHC Run 2 safe points.

EW symmetry, led to *barely-broken* EW symmetry. This is the same as the naturalness condition that $m_{H_u}^2$ is driven to small negative values at the weak scale, and so gave a *mechanism* for why $m_{H_u}^2$ should be driven to natural values. It was also emphasized that the statistical draw to large soft terms must avoid CCB and no EWSB vacua while at the same time drawing towards a weak scale not too far from its measured value. The combined statistical/anthropic draw would pull soft terms towards a region where A_t is large (but not too large) and where $m_h \sim 125$ GeV.

In Ref. [18], previous work by DD was adopted wherein soft SUSY breaking terms were actually selected according to $f_{SUSY} \sim m_{soft}^n$ with $n = 2n_F + n_D - 1$ while f_{EWSB} was adopted as in Eq. 6. This allowed for *landscape probability distributions* to be calculated for a host of superparticle and Higgs masses. Calculations were performed using the three-extra parameter non-universal Higgs model (NUHM3) with parameter space given by

$$m_0(1,2), m_0(3), m_{1/2}, A_0, \tan\beta, \mu, m_A \quad (\text{NUHM3}) \quad (9)$$

where separate first/second and third generation soft scalar masses and a negative A_0 term were used. For $n = 1$ or 2, then the differential probability distribution for the Higgs mass dP/dm_h acquired a firm peak around $m_h \sim 125$ GeV.

Results from a scan over soft terms with $\mu : 100 - 360$ GeV with $A_0 < 0$ and $n = 1$ (corresponding to a single SUSY breaking field F) are shown in Fig. 2 for the case where the generated weak scale is less than a factor four from its measured value. The green histogram shows results when LHC search constraints (except Higgs mass) are also imposed (see below).

Furthermore, the probability distributions for other sparticle masses gave

- $m_{\tilde{g}} \sim 4 \pm 2$ TeV,
- $m_{\tilde{t}_1} \sim 1.5 \pm 0.5$ TeV,

- $m_A \sim 3 \pm 2$ TeV,
- $\tan \beta \sim 13 \pm 7$,
- $m_{\tilde{\chi}_1^\pm, \tilde{\chi}_{1,2}^0} \sim 200 \pm 100$ GeV,
- $m_{\tilde{\chi}_2^0} - m_{\tilde{\chi}_1^0} \sim 7 \pm 3$ GeV and
- $m_{\tilde{q}, \tilde{\ell}} \sim 20 \pm 10$ TeV.

From these results, one may conclude that the present LHC Run 2 results of finding a SM-like Higgs boson with $m_h = 125$ GeV and no sign of sparticles is seeing exactly that which the landscape with $n = 1$ or 2 predicts will be seen. Furthermore, the higgsino-like WIMPs would form only a portion of dark matter (along with a SUSY DFSZ-like axion). Since the higgsino-like WIMPs typically constitute only $\sim 10\%$ of dark matter, their detection rates lie below present WIMP search limits.

We also have checked the case with positive A term. Sparticles are pulled to higher masses due to the statistical draw but the Higgs mass peaks at 120 GeV and less than 1% of the scan points give correct Higgs mass. Since our main motivation for the landscape picture is the prediction of m_h at its measured value, we do not consider experimental implications of $A_0 > 0$ for the remainder of the paper.

Our goal for the present paper is to confront the panoply of recent LHC and WIMP search experiment results with the predictions from the string theory landscape.

3 Landscape predictions vs. LHC search limits

In this Section, we confront the string theory landscape predictions for $n = 1$ with LHC sparticle search constraints and projected reach limits.

3.1 Landscape predictions for NUHM2 model

In years past, it was common to portray collider search limits in the $m_{1/2}$ vs. m_0 plane of the mSUGRA/CMSSM model [27, 28]. In this model, the matter and Higgs soft mass terms are unified to a common GUT scale value m_0 , where the GUT scale is defined as that scale $m_{GUT} \simeq 2 \times 10^{16}$ GeV where the gauge couplings g_1 and g_2 unify. In the mSUGRA/CMSSM model, since $m_{H_u}^2 = m_{H_d}^2 \equiv m_0^2$ as an input parameter, then μ is constrained by Eq. 7 so as to ensure the measured value of $m_Z = 91.2$ GeV. The natural portion of parameter space using Barbieri-Giudice fine-tuning [29] was found to be the lowest allowed values of m_0 and $m_{1/2} \lesssim 200$ GeV [30]. This region is long-since excluded by LHC sparticle search constraints which with 80 fb^{-1} of integrated luminosity now require $m_{\tilde{g}} \gtrsim 2.25$ TeV and $m_{\tilde{t}_1} \gtrsim 1.1$ TeV.

The value of μ in the LHC-allowed region is only natural $\sim 100 - 300$ GeV in the focus point (FP) region [31]. But the FP region appears only for the smaller range of A_0 where m_h is too low [32]. Thus, the region of mSUGRA/CMSSM parameter space with $m_h \sim 123 - 127$ GeV is always highly fine-tuned [33]. For this reason, we work instead first in the two-extra-parameter non-universal Higgs model NUHM2 [34] which allows independent input values of $m_{H_u}^2$ and

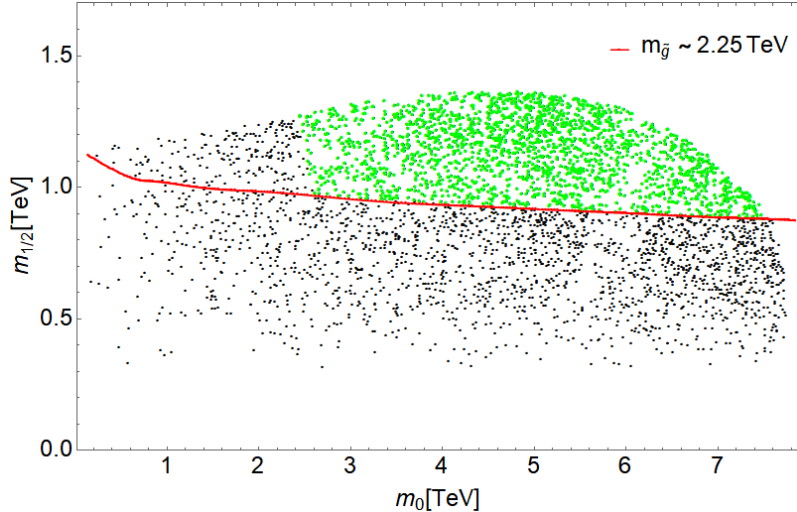


Figure 3: Locus of $n = 1$ landscape scan points for the NUHM2 model with $\mu = 200$ GeV in the $m_{1/2}$ vs. m_0 plane along with recent LHC Run2 constraints for $A_0 = -1.6m_0$, $m_A = 2$ TeV and $\tan\beta = 10$. The soft terms m_0 and $m_{1/2}$ are selected with $n = 1$ and $\Delta_{\text{EW}} < 30$ so that the weak scale is within ~ 4 of its measured value. The red contour corresponds to the LHC Run 2 limit that $m_{\tilde{g}} \gtrsim 2.25$ TeV. Green points are allowed by LHC Run 2 constraints (see text) while black points are excluded by LHC Run 2.

$m_{H_d}^2$ (since the Higgs live in independent GUT multiplets anyway). The values of $m_{H_u}^2$ and $m_{H_d}^2$ may be traded for weak scale inputs μ and m_A . This allows us to adopt a natural value of $\mu \simeq 200$ GeV over all parameter space. We use Isajet 7.88 for our SUSY spectra generation and calculation of Δ_{EW} [35].

In Fig. 3 we display the $m_{1/2}$ vs. m_0 plane of the NUHM2 model for $\mu = 200$ GeV, $\tan\beta = 10$, $A_0 = -1.6m_0$ and $m_A = 2$ TeV. The soft terms m_0 and $m_{1/2}$ are generated randomly for $m_0 : 0 \rightarrow 10$ TeV and $m_{1/2} : 0.3 - 3$ TeV but with the $n = 1$ increasing distribution and $\Delta_{\text{EW}} < 30$ so that the weak scale is within ~ 4 of its measured value. We see that the low m_0 and $m_{1/2}$ region is now sparsely populated due to the (mild) draw of the landscape towards large soft terms. In this plot, the density of points actually reflects the assumed vacuum statistics of the landscape with $n = 1$. The density increases with increasing m_0 and $m_{1/2}$ until the points cut off where soft term contributions to the weak scale exceed the measured weak scale by a factor four ($\Delta_{\text{EW}} > 30$). The red line denotes the latest LHC Run 2 bound of $m_{\tilde{g}} \gtrsim 2.25$ TeV. The green points are LHC-allowed while black points above the red contour at lower m_0 have $m_h < 123$ GeV (we assume an approximate ± 2 GeV theory error in the Isajet m_h calculation). The green LHC-allowed points range up to $m_{\tilde{g}} \sim 3.5$ TeV although for other parameter choices and moving to the NUHM3 model then gluinos can range as high as 6 TeV [36]. The most densely populated region of parameter space remains beyond current LHC reach and it may require an upgrade to high energy LHC (HE-LHC with $\sqrt{s} = 27$ TeV and 15 ab^{-1} of integrated luminosity) to completely cover the remaining parameter space in the gluino pair production search channel [37].

3.2 Landscape predictions for NUHM3 model

In this Subsection, we investigate landscape predictions within the more general NUHM3 model where first/second generation matter scalars have different soft terms from third generation matter scalars. This sort of setup is motivated in part by investigations of the minilandscape of heterotic string models compactified on an orbifold [38]. In these models, the first/second generation multiplets live near orbifold fixed points and obey localized grand unification [39]: they live in the 16-dimensional spinor reps of $SO(10)$. In contrast, the third generation matter scalars, Higgs multiplets and gauginos live more in the bulk of the compactified orbifold and hence live in the usual SM split multiplets.

In this section, we will scan over soft parameters as $m_{\text{soft}}^{n=1}$ with the following ranges:

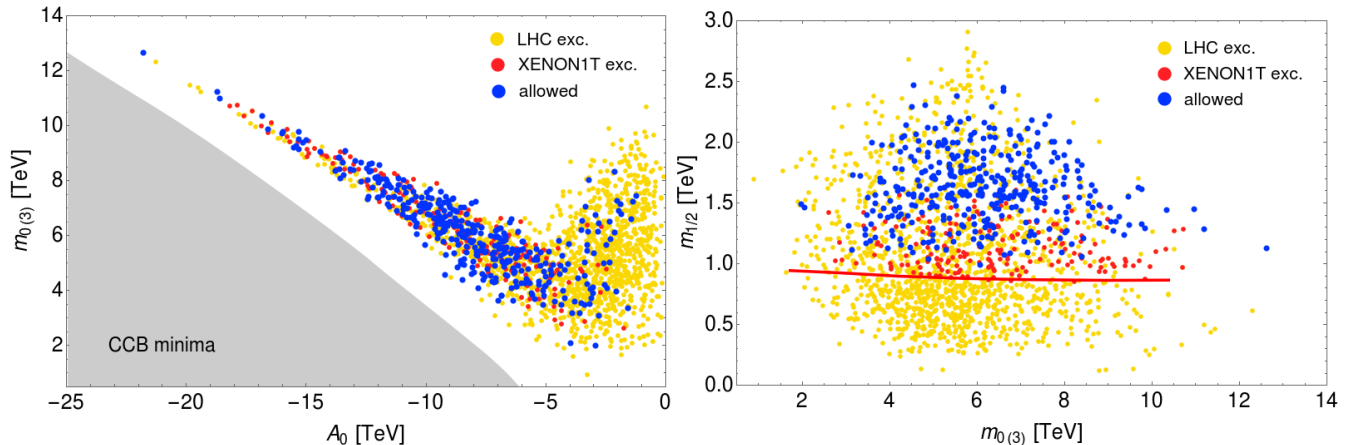
- $m_0(1, 2) : 0 - 55$ TeV,
- $m_0(3) : 0 - 20$ TeV,
- $m_{1/2} : 0 - 3.2$ TeV,
- $-A_0 : 0 - 25$ TeV and
- $m_A : 0 - 10$ TeV,

while we scan over $\tan \beta : 3 - 60$ and $\mu : 100 - 360$ GeV uniformly since $\tan \beta$ is not dimensional and μ arises from our assumed solution to the SUSY μ problem. The lower limit of the μ term comes from the LEP2 limit on the lightest chargino mass, $\tilde{\chi}_1^\pm > 103.5$ GeV. We again require an appropriate EWSB and further require no contributions of Eq. 7 to the weak scale to exceed a factor four (*i.e.* $\Delta_{\text{EW}} < 30$).

Our first results are shown in Fig. 4a where we show scan points in the $m_0(3)$ vs. A_0 plane. Here we divide our scan points into three sets. Yellow points are excluded by recent LHC Run 2 search limits:

- $m_{\tilde{g}} \gtrsim 2.25$ TeV for $\tilde{g} \rightarrow t\bar{t} + \tilde{\chi}_1^0$ [40],
- $m_{\tilde{t}_1} \gtrsim 1.1$ TeV for $\tilde{t} \rightarrow t^{(*)} + \tilde{\chi}_1^0$ [41],
- bounds from $H/A \rightarrow \tau^+\tau^-$ in the $\tan \beta$ vs. m_A plane [42],
- higgsino pair production [43]: points are beyond the recent LHC soft dilepton+jets+ \cancel{E}_T constraints (shown later in Fig. 8b),
- $m_h = 125 \pm 2$ GeV (to account for theory error of the calculation)

The blue shaded points have acceptable vacua and obey both LHC and WIMP search constraints. The red points are LHC-allowed but excluded by recent XENON1T spin-independent (SI) direct WIMP detection (DD) searches [44] (see later Fig. 10). The main lesson from Fig. 4a is that the acceptable points lie in a very restricted regions where $m_0(3)$ and $-A_0$ are correlated: if A_0 gets too large (negative), then the model is forced into CCB minima so the gray region is disallowed. Likewise, if for fixed A_0 then $m_0(3)$ gets too large, then third generation



(a) We show regions of $\Delta_{EW} > 30$ (blank) and CCB minima (lower left) in the scalar potential. The blue points are LHC Run 2 and DM-allowed.

(b) LHC Run 2 limit for $m_{\tilde{g}} > 2.25$ TeV is shown by the red contour.

Figure 4: Locus of $n = 1$ landscape scan points in the (a) $m_{0(3)}$ vs. A_0 and (b) $m_{1/2}$ vs. $m_{0(3)}$ planes for the NUHM3 model with $\mu = 100 - 360$ GeV.

contributions to the weak scale $\Sigma_u^u(\tilde{t}_{1,2})$ exceed the measured weak scale by over a factor four (blank region).

In Fig. 4b we show the $m_{1/2}$ vs. $m_{0(3)}$ soft term plane. The LHC Run 2 requirement that $m_{\tilde{g}} \gtrsim 2.25$ TeV is shown by the red contour. There are plenty of surviving landscape scan points with $m_{1/2}$ ranging from 1 – 2.5 TeV. The upper range of allowed $m_{1/2}$ values correspond to values of $m_{\tilde{g}}$ over 6 TeV. Few scan points exist for $m_{0(3)} \lesssim 2$ TeV since the $n = 1$ scan prefers linearly increasing soft terms. Few points also exist for $m_{0(3)} \gtrsim 12$ TeV since these points would give too large $\Sigma_u^u(\tilde{t}_{1,2})$ contributions to the weak scale.

In Fig. 5a, we show our $n = 1$ landscape scan points in the $m_{\tilde{\chi}_1^0}$ vs. $m_{\tilde{g}}$ plane which is the usual simplified model plane in which LHC gluino searches are usually presented. The current LHC Run 2 exclusion contour based on 80 fb^{-1} of integrated luminosity is shown as the black contour. It is also interesting that the XENON1T dark matter search excludes significant regions of the lighter LSP masses for gluino masses of order 2 – 3.5 TeV. HL-LHC will be able to cover points with gluinos only up to 2.8 TeV via the gluino pair production channel [45]. We also show the recently computed 95% CL HE-LHC projected search limit for $\sqrt{s} = 27$ TeV and 15 ab^{-1} which reaches to $m_{\tilde{g}} \sim 6$ TeV. Evidently a complete examination of $n = 1$ landscape points in the $\tilde{g}\tilde{g}$ search channels will require HE-LHC.

In Fig. 5b, we show $n = 1$ landscape points in the $m_{\tilde{\chi}_1^0}$ vs. $m_{\tilde{t}_1}$ simplified model plane. The current LHC Run 2 search limits are shown as the black contour. There is a high density of LHC-allowed (blue) points extending from $m_{\tilde{t}_1} \sim 1.1$ to 2.7 TeV. The projected reach of HL-LHC with $\sqrt{s} = 14$ TeV and 3 ab^{-1} extends to $m_{\tilde{t}_1} \sim 1.7$ TeV and covers perhaps the greatest density of blue points. Nonetheless, it will require an upgrade to HE-LHC to cover the complete set of $n = 1$ landscape points [37].

In Fig. 6, we show the $n = 1$ landscape points in the $m_{\tilde{g}}$ vs. $m_{\tilde{t}_1}$ plane. Of note here is that

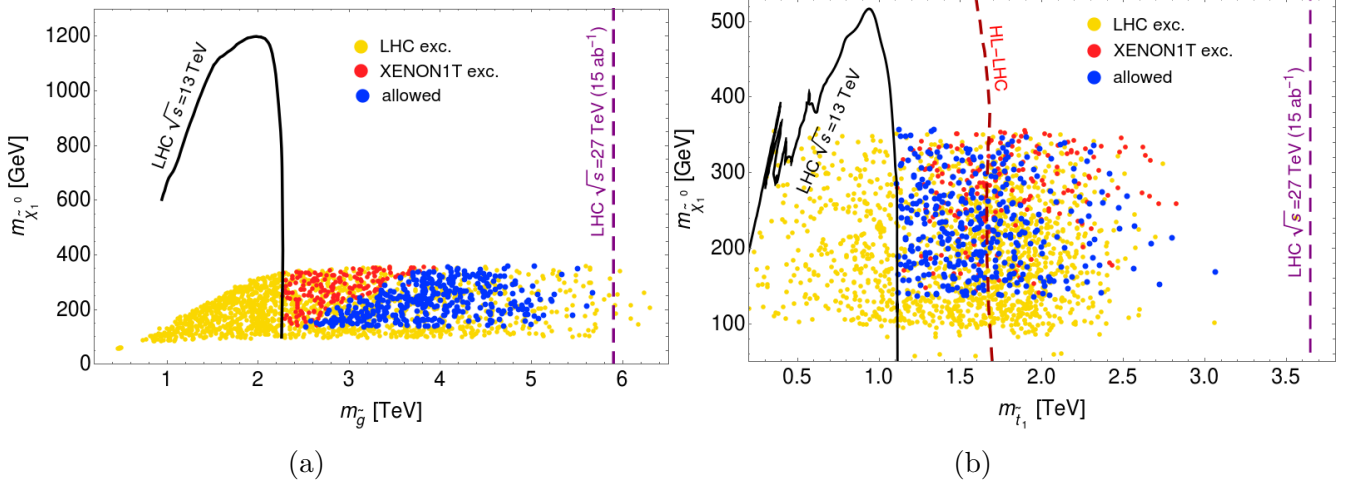


Figure 5: Locus of $n = 1$ landscape scan points for the NUHM3 model with $\mu = 100 - 360$ GeV in the (a) $m_{\tilde{\chi}_1^0}$ vs. $m_{\tilde{g}}$ and (b) $m_{\tilde{\chi}_1^0}$ vs. $m_{\tilde{t}_1}$ planes versus recent LHC Run2 constraints.

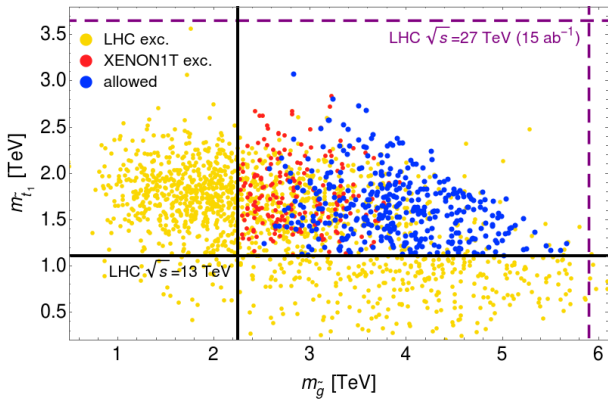


Figure 6: Locus of $n = 1$ landscape scan points for the NUHM3 model with $\mu = 100 - 360$ GeV in the $m_{\tilde{t}_1}$ vs. $m_{\tilde{g}}$ plane versus recent LHC Run2 constraints (black) and projected HE-LHC 95% CL reach contours (purple-dashed).

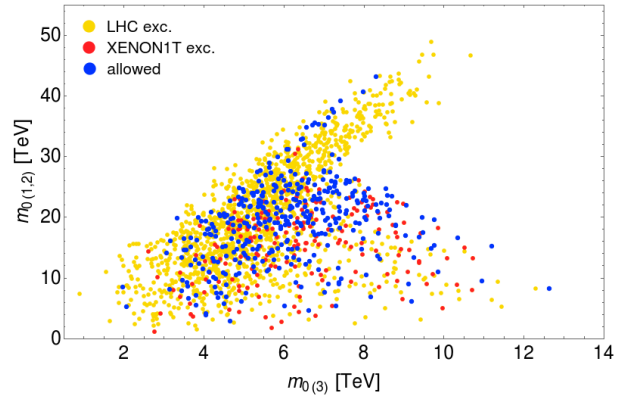


Figure 7: Locus of $n = 1$ landscape scan points for the NUHM3 model in the $m_{0(1,2)}$ vs. $m_{0(3)}$ plane for $\mu = 100 - 360$ GeV.

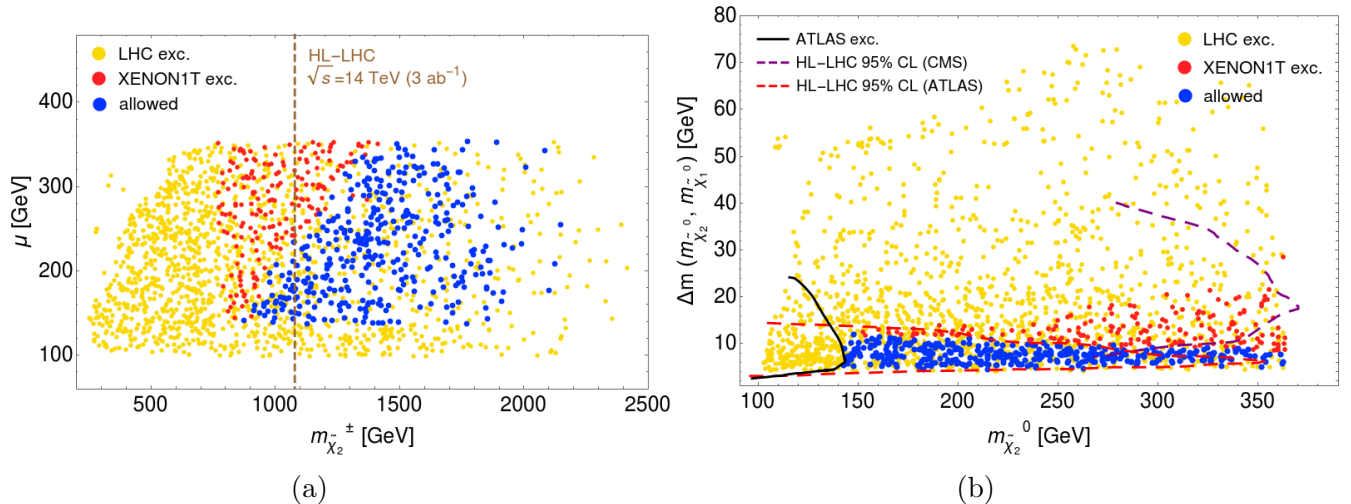


Figure 8: Locus of $n = 1$ landscape scan points for the NUHM3 model with $\mu = 100 - 360$ GeV in the (a) μ vs. $m_{\tilde{\chi}_2^\pm}$ and (b) $m_{\tilde{\chi}_2^0} - m_{\tilde{\chi}_1^0}$ vs. $m_{\tilde{\chi}_2^0}$ planes versus projected HL-LHC 95% CL search limits.

the points with the largest values of $m_{\tilde{g}}$ have the smaller range of $m_{\tilde{t}_1}$ and vice-versa. Thus, if somehow for instance gluinos were able to escape LHC detection on account of them being too heavy, the top squarks would surely be seen (and vice-versa). A complete coverage of the $n = 1$ landscape parameter space will require HE-LHC with 15 ab^{-1} of integrated luminosity.

In Fig. 7, we show the $m_0(1,2)$ vs. $m_0(3)$ plane of the NUHM3 model for the $n = 1$ landscape. The important lesson from this plot is that first/second generation matter scalar soft terms tend to inhabit the 10-30 TeV range whilst third generation matter scalar soft terms lie typically below 10 TeV. RG and mixing effects then cause the third generation squarks/sleptons to lie in the few TeV range (so their loop-suppressed contributions Σ_u^u to the weak scale are small) while first/second generation squarks and slepton (with mass $m_{\tilde{q},\tilde{l}} \sim m_0(1,2)$) lie well beyond even HE-LHC reach and offer at least a partial decoupling solution to the SUSY flavor and CP problems. The reason they can be so heavy is that the first/second generation sfermion contributions to the weak scale are D -term contributions which largely cancel [46].

Another important LHC search plane is the μ vs. $m_{\tilde{\chi}_2^\pm}$ plane. This plane is important for presenting search limits from same-sign diboson (SSdB) production arising from wino pair production in SUSY models with light higgsinos. The reaction is $pp \rightarrow \tilde{\chi}_2^\pm \tilde{\chi}_4^0$ where $\tilde{\chi}_2^\pm \rightarrow W^\pm \tilde{\chi}_{1,2}^0$ while $\tilde{\chi}_4^0 \rightarrow W^\mp \tilde{\chi}_1^\pm$ so that half the time one arrives at a final state with two same-sign W bosons plus large \cancel{E}_T . For leptonically-decaying W bosons, then the final state consists of a same-sign dilepton + \cancel{E}_T signature which is relatively jet free- in contrast to same-sign dileptons originating from gluino and squark pair production. The same-sign channel has rather tiny SM backgrounds [47–49]. So far, no search results have been presented by ATLAS or CMS. From Fig. 8a, we see that LHC-allowed points only begin at wino masses $m_{\tilde{\chi}_2^\pm} \sim 800$ GeV and then extend out to $m_{\tilde{\chi}_2^\pm} \sim 2300$ GeV. This is to be compared with the projected HL-LHC 95% CL search limit which is the brown contour reaching to $m_{\tilde{\chi}_2^\pm} \sim 1100$ GeV [49]. Projected search limits for HE-LHC in the SSdB channel have yet to be computed.

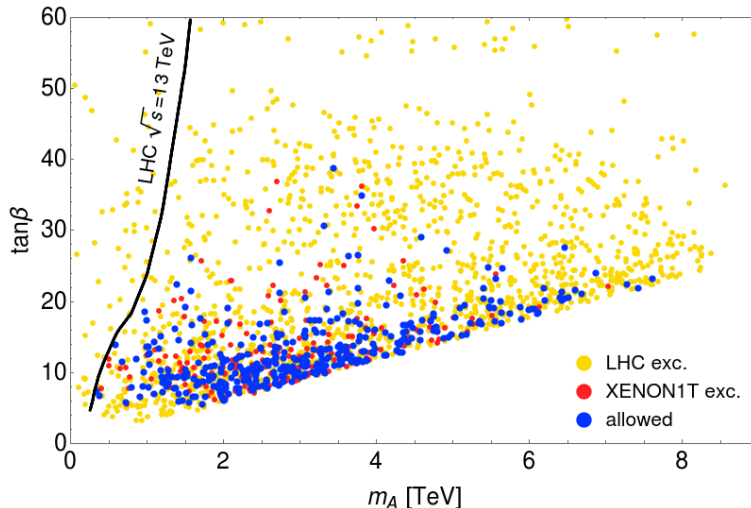


Figure 9: Locus of $n = 1$ landscape scan points for the NUHM3 model with $\mu = 100 - 360$ GeV in the $\tan\beta$ vs. m_A plane versus recent LHC Run2 constraints. Blue points are LHC Run 2 and DM-allowed while red points are LHC-safe but excluded by XENON1T WIMP search limits.

In Fig. 8b, we show the $n = 1$ landscape points in the $\Delta m \equiv m_{\tilde{\chi}_2^0} - m_{\tilde{\chi}_1^0}$ vs. $m_{\tilde{\chi}_2^0}$ plane. This plane is important for the light higgsino pair production searches $pp \rightarrow \tilde{\chi}_2^0 \tilde{\chi}_1^0$ (and $\tilde{\chi}_2^0 \tilde{\chi}_1^\pm$) where $\tilde{\chi}_2^0 \rightarrow \ell^+ \ell^- \tilde{\chi}_1^0$ giving rise to a soft opposite-sign dilepton pair whose invariant mass is bounded by $m_{\tilde{\chi}_2^0} - m_{\tilde{\chi}_1^0}$ [50]. To trigger on such events, it seems necessary to require a hard jet radiation from the initial state against which the soft dileptons can recoil. Recent search limits have been presented by both ATLAS [43] and CMS [51]. We show as a black contour the recent ATLAS limit. An important point of the $n = 1$ landscape is that it favors heavier gauginos while μ must not be too far from the weak scale. The combination squeezes down the inter-higgsino mass gap $m_{\tilde{\chi}_2^0} - m_{\tilde{\chi}_1^0}$ so that in this case all the LHC-allowed points have $\Delta m \lesssim 10$ GeV. We also show recently computed projected HL-LHC 95% CL reach contours [52]. The ATLAS contour has focussed on the small mass gap region and appears to cover nearly all parameter space. This has important implications for how SUSY is likely to be revealed at LHC. Gluinos and top squarks are expected to be drawn to large values, possibly beyond HL-LHC reach. The soft dilepton plus jet + \cancel{E}_T channel (SDLJMET) is the only channel that seems to be (nearly) completely covered by HL-LHC. Thus, we would expect a SUSY signal in this channel to emerge slowly but conclusively during the next 15 years as LHC acquires its full complement of 3 ab^{-1} of integrated luminosity!

A final natural SUSY search channel occurs in the Higgs sector by looking for $pp \rightarrow A, H \rightarrow \tau^+ \tau^-$ events. These searches are typically presented in the $\tan\beta$ vs. m_A plane which we show in Fig. 9. We also show the recent LHC excluded region as the black contour [42]. This latter contour assumes only SM decay modes for the A and H but for the landscape then the decay modes $H, A \rightarrow \text{higgsinos}$ should almost always be open as well (and might lead to $4\ell + \cancel{E}_T$ signatures [53]). The added $H, A \rightarrow \text{higgsinos}$ decay modes hardly affect the search limits since a diminution of Higgs to SM branching fractions can be offset by increasing the Higgs

production cross sections by moving to somewhat larger $\tan\beta$ [54]. From the plot, we see that the LHC-allowed points are typically well beyond the current LHC reach limits and the greatest density populates the region of $m_A \sim 2 - 5$ TeV and at lower $\tan\beta$ values where $b\bar{b}$ fusion contributions to the production cross section are not so big. Thus, we see only a small likelihood of a signal emerging in this channel at LHC.

4 Landscape predictions vs. WIMP DM search limits

In $n = 1$ landscape SUSY, we expect soft terms to be drawn to large values whilst the μ term is not too far from the weak scale. This results in a Little Hierarchy (LH) with $\mu \ll m_{soft}$ which turns out to be non-problematic. In such a scenario, then the lightest SUSY particle is the lightest higgsino-like neutralino with mass $m_{\tilde{\chi}_1^0} \sim 90 - 360$ GeV. These natural higgsino-like WIMPs are thermally underproduced as dark matter, which may be a reason why they had not been considered much previous to 2011 [55–57]. However, one must recall that the QCD sector of the SM also suffers a naturalness issue in the form of the strong CP problem. Including an axion sector into the MSSM is thus well-motivated both for solving the strong CP problem but also to solve the SUSY μ problem (for a recent review, see *e.g.* Ref. [58]) via a DFSZ-type SUSY axion. Thus, in natural SUSY it is expected that the DM is a WIMP-axion admixture (*i.e.* two dark matter particles). If the natural SUSY WIMPs (with $m_{\tilde{\chi}_1^0} \lesssim 350$ GeV) were *all* of DM, then they would actually be excluded by current WIMP search constraints [59]. But if the DM is mainly axions, then there are far fewer relic WIMPs present in the cosmos and they can escape present limits from WIMP search experiments. A full evaluation of mixed WIMP-axion dark matter requires an eight-coupled Boltzmann equation evaluation which accounts also for axino, saxion and gravitino production and decay in the early universe [60].

We first examine WIMP search limits via ton-scale noble liquid experiments using targets such as Xenon or Argon. To compare WIMP search limits to landscape projections, one must calculate $\xi\sigma^{SI}(\tilde{\chi}_1^0, p)$ where $\xi \equiv \Omega_{\tilde{\chi}_1^0} h^2 / 0.12$, *i.e.* it is the fractional abundance of WIMPs in making up the totality of dark matter. Usually this is just the WIMP thermal abundance divided by the measured abundance although it is possible the WIMP abundance is supplemented by non-thermal processes such as axino or saxion decay in the early universe.

In Fig. 10, we plot the locus of $n = 1$ landscape points in the $\xi\sigma^{SI}(\tilde{\chi}_1^0, p)$ vs. $m_{\tilde{\chi}_1^0}$ plane. We also show current search limits from the XENON-100 experiment [61] (black contour) and the XENON1T experiment [44] (red contour). A subset of LHC-allowed points are already excluded, and denoted as red points. However, the bulk of $n = 1$ landscape points are still allowed, and extend down to an order of magnitude below present limits. These points do not extend all the way to the neutrino floor since in SUSY the WIMPs couple to nucleons mainly via light Higgs exchange and this coupling involves a production of gaugino times higgsino components [57]. In natural SUSY, the WIMP is mainly higgsino, but with non-negligible gaugino component (lest heavy gauginos give too large a contribution to the weak scale). Thus, it appears that projected search limits from XENONnT (multi-ton Xenon detector), LUX-ZEPLIN (LZ) [62] and other multi-ton-scale detectors [63] should cover the entire $n = 1$ landscape parameter space, even if WIMPs comprise only a portion of the dark matter.

In Fig. 11a, we show the spin-dependent (SD) direct detection scattering rate $\xi\sigma^{SD}(\tilde{\chi}_1^0, p)$

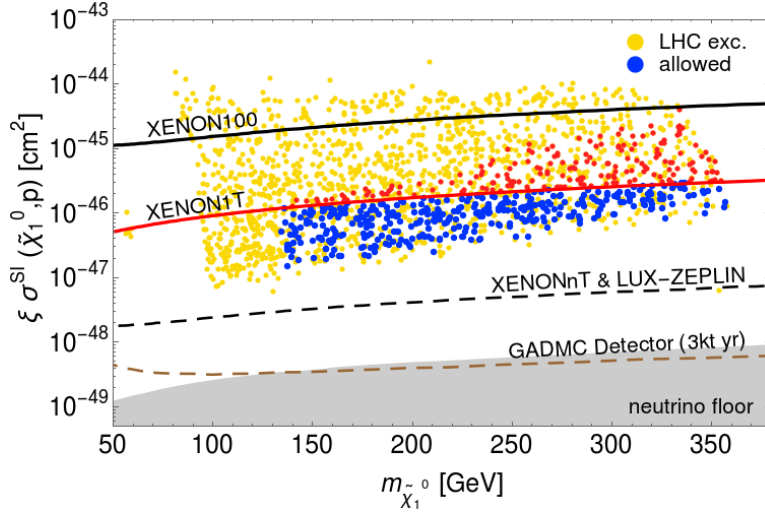
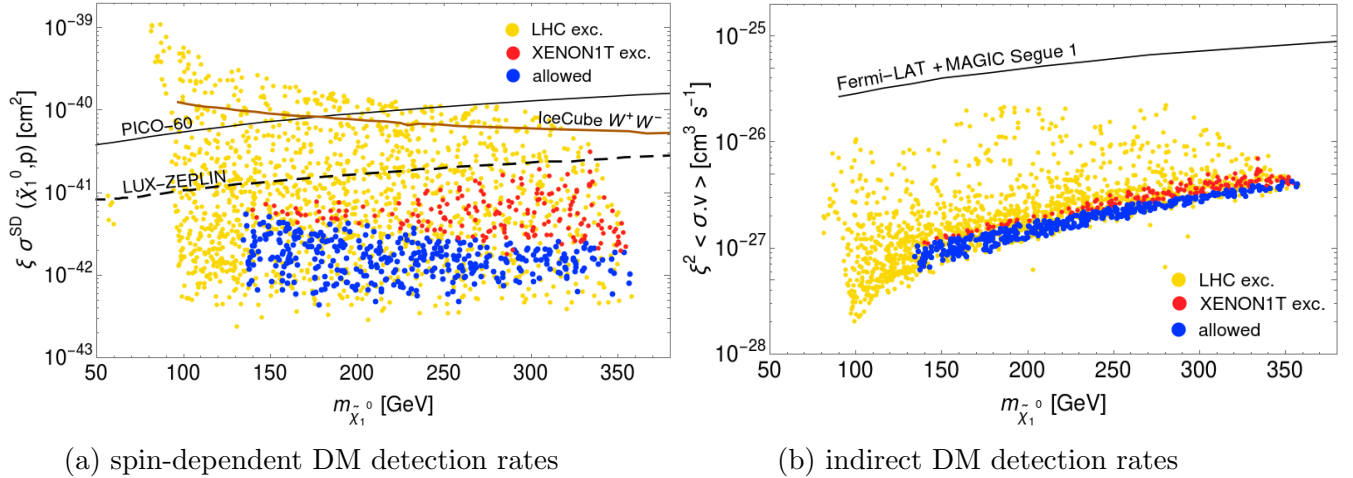


Figure 10: Locus of $n = 1$ landscape scan points for the NUHM3 model in the $\xi\sigma^{SI}(\tilde{\chi}_1^0, p)$ vs. $m_{\tilde{\chi}_1^0}$ plane versus recent WIMP search constraints for $\mu = 100 - 360$ GeV. Red points are excluded by XENON1T search limits but not by LHC Run 2 constraints. Projected reaches from several future SI DD experimentes are also shown.



(a) spin-dependent DM detection rates

(b) indirect DM detection rates

Figure 11: Locus of $n = 1$ landscape scan points for the NUHM3 model with $\mu = 100 - 360$ GeV in the (a) $\xi\sigma^{SD}(\tilde{\chi}_1^0, p)$ vs. $m_{\tilde{\chi}_1^0}$ and (b) $\xi^2\langle\sigma v\rangle$ vs. $m_{\tilde{\chi}_1^0}$ planes versus recent WIMP search constraints.

vs. $m_{\tilde{\chi}_1^0}$ plane along with projected $n = 1$ landscape rates. We also show recent limits from the PICO-60 experiment [64] and IceCube in the W^+W^- annihilation mode [65]. In this case, the LHC-allowed landscape points tend to lie about an order of magnitude below the current limits. We also show the projected future reach of LZ [62]. Even this contour does not quite reach the expected theory region.

In Fig. 11b, we show the indirect WIMP detection rates (IDD) in the $\xi^2 \langle \sigma \cdot v \rangle$ vs. $m_{\tilde{\chi}_1^0}$ plane, where ξ^2 is required since these signals arise from WIMP-WIMP annihilation in the cosmos and is thus suppressed by the fractional WIMP abundance squared. We show also the recent Fermi-LAT+Magic limits from observation of dwarf spheroidal galaxy Segue-1 [66]. The current limit is over an order of magnitude above the expected LHC-allowed points from the $n = 1$ landscape. A signal from the IDD search channel would point to non-thermal production of WIMPs (*i.e.* from decays of axinos/saxions) in addition to the thermally-produced neutralinos.

5 Conclusions

Rather general arguments regarding the statistics of the landscape of flux vacua in string theory point to a statistical draw towards large soft SUSY breaking terms governed by a power law m_{soft}^n where $n = 2n_F + n_D - 1$ involves the number of F and D term SUSY breaking fields in a (possibly) complicated hidden sector. With only the draw towards large soft terms, one would expect a huge value for the weak scale since m_{weak} is determined by the visible sector soft terms and the SUSY μ parameter. A huge weak scale would mean highly suppressed weak interactions and huge particle masses which would likely lead to a non life-supporting universe. Agrawal *et al.* calculated that an increase in m_{weak} by a factor of ~ 3 would lead to a non-livable universe. Therefore, we have tempered the statistical draw of the landscape to large soft terms with the anthropic requirement of a weak scale no more than (conservatively) four times its measured value. For a fixed natural value of μ (arising from some solution to the SUSY μ problem such as hybrid CCK which also solves the strong CP problem and introduces axionic along with higgsino-like WIMP dark matter [26]), then one may implement random scans over power-law increasing soft terms tempered by an anthropic requirement of the weak scale not too far from $m_{weak} \sim 100$ GeV. The cases for $n = 1$ and 2 lead to a landscape probability distribution for the light Higgs mass which peaks around ~ 125 GeV. Also, most superparticle masses are pulled to large values beyond LHC reach. In this case, *LHC sparticle and WIMP dark matter search experiments are seeing exactly that which is expected from the $n = 1, 2$ landscape*: a Higgs mass of 125 GeV and no sign yet of sparticles.

Our goal in this paper was a practical one: place the $n = 1$ landscape statistical predictions on the same plots that LHC sparticle and WIMP dark matter search experiments use in order to assess where sparticle and WIMP masses might be located relative to present and future search limits. In these sorts of plots, the density of points actually has meaning since it would reflect the assumed statistics of string theory vacua in a fertile patch which includes the MSSM as the weak scale effective theory.

Our findings are that strongly interacting sparticles \tilde{g} and \tilde{t}_1 are likely to lie beyond present LHC search bounds and possibly beyond HL-LHC projected search limits. It may require an upgrade to HE-LHC to cover the entire $n = 1$ landscape parameter space in the $\tilde{g}\tilde{g}$ and $\tilde{t}_1\tilde{t}_1^*$

modes as manifested in the context of the natural NUHM3 SUSY model. Also, the SSdB signal may or may not be detected by HL-LHC and the $A, H \rightarrow \tau^+\tau^-$ signals are likely to lie well beyond the reach of LHC upgrades. However, the SDLJMET signal arising from higgsino pair production offers a search channel wherein HL-LHC may cover the entire projected parameter space. In this case, we would expect a SUSY signal to emerge slowly but conclusively by ATLAS and CMS as more and more integrated luminosity accrues.

Regarding WIMP searches, it appears that a full complement of data from multi-ton noble liquid SI direct detection experiments should cover the entire $n = 1$, NUHM3 landscape parameter space. This can occur even though in natural SUSY the higgsino-like WIMPs make up only a portion of dark matter with SUSY DFSZ axions making up the remainder. Meanwhile, even upgraded SD detectors may well fall short of covering the portion of parameter space occupied by the $n = 1$ landscape model. It appears that IDD WIMP search experiments will also have a hard time accessing the full parameter space since now the expected signal rates are diminished by the square of the fractional WIMP abundance. The search for SUSY DFSZ axions, addressed in Ref. [67], is also difficult due to the presence of higgsinos circulating in the $a\gamma\gamma$ coupling diagram: they tend to suppress the DFSZ axion coupling to much lower values than are typically displayed in axion search result plots.

To summarize:

- The $n = 1$ landscape statistics predict $m_h \sim 125$ GeV with superparticles beyond the reach of present LHC and WIMP DD experiments.
- LHC signals in SDLJMET channel should emerge slowly as LHC attains higher and higher integrated luminosity. A signal should likely be seen with 3 ab^{-1} at HL-LHC if not sooner. Signals in other channels such as $\tilde{g}\tilde{g}$, $\tilde{t}_1\tilde{t}_1^*$ and SSdB may emerge at HL-LHC if we are lucky but otherwise may require an upgrade to HE-LHC.
- WIMP detection signals should emerge in SI DD experiments using multi-ton noble liquids. Signals in SD DD or IDD are much less likely to emerge in the near future.

Acknowledgements: We thank Art McDonald for discussions on future WIMP detectors. This work was supported in part by the US Department of Energy, Office of High Energy Physics. The computing for this project was performed at the OU Supercomputing Center for Education & Research (OSCER) at the University of Oklahoma (OU).

References

- [1] R. Bousso and J. Polchinski, JHEP **0006** (2000) 006.
- [2] L. Susskind, In *Carr, Bernard (ed.): Universe or multiverse?* 247-266 [hep-th/0302219].
- [3] R. Bousso and J. Polchinski, Sci. Am. **291** (2004) 60.
- [4] S. Weinberg, Phys. Rev. Lett. **59** (1987) 2607; S. Weinberg, Rev. Mod. Phys. **61** (1989) 1.
- [5] M. R. Douglas, JHEP **0305** (2003) 046; S. Ashok and M. R. Douglas, JHEP **0401** (2004) 060.

- [6] S. Weinberg, In *Carr, Bernard (ed.): Universe or multiverse?* 29-42 [hep-th/0511037].
- [7] V. Agrawal, S. M. Barr, J. F. Donoghue and D. Seckel, Phys. Rev. D **57** (1998) 5480; V. Agrawal, S. M. Barr, J. F. Donoghue and D. Seckel, Phys. Rev. Lett. **80** (1998) 1822.
- [8] M. R. Douglas, Comptes Rendus Physique **5** (2004) 965 doi:10.1016/j.crhy.2004.09.008 [hep-th/0409207].
- [9] L. Susskind, In *Shifman, M. (ed.) et al.: From fields to strings, vol. 3* 1745-1749 [hep-th/0405189].
- [10] F. Denef and M. R. Douglas, JHEP **0405**, 072 (2004).
- [11] M. R. Douglas, hep-th/0405279.
- [12] M. R. Douglas, Les Houches Lect. Notes **97** (2015) 315.
- [13] M. Dine, E. Gorbatov and S. D. Thomas, JHEP **0808** (2008) 098; for reviews, see M. Dine, hep-th/0410201.
- [14] F. Denef, M. R. Douglas and S. Kachru, Ann. Rev. Nucl. Part. Sci. **57** (2007) 119.
- [15] J. Kumar, Int. J. Mod. Phys. A **21** (2006) 3441.
- [16] H. P. Nilles, Phys. Rept. **110** (1984) 1.
- [17] N. Arkani-Hamed and S. Dimopoulos, JHEP **0506** (2005) 073.
- [18] H. Baer, V. Barger, H. Serce and K. Sinha, JHEP **1803** (2018) 002.
- [19] J. A. Casas, A. Lleyda and C. Munoz, Nucl. Phys. B **471** (1996) 3.
- [20] H. Baer, M. Brhlik and D. Castano, Phys. Rev. D **54** (1996) 6944.
- [21] G. F. Giudice and R. Rattazzi, Nucl. Phys. B **757** (2006) 19.
- [22] H. Baer, V. Barger, M. Savoy and H. Serce, Phys. Lett. B **758** (2016) 113.
- [23] H. Baer, V. Barger, P. Huang, A. Mustafayev and X. Tata, Phys. Rev. Lett. **109**, 161802 (2012).
- [24] H. Baer, V. Barger, P. Huang, D. Mickelson, A. Mustafayev and X. Tata, Phys. Rev. D **87**, 115028 (2013).
- [25] H. Baer and X. Tata, “Weak scale supersymmetry: From superfields to scattering events,” Cambridge, UK: Univ. Pr. (2006) 537 p.
- [26] H. Baer, V. Barger and D. Sengupta, Phys. Lett. B **790** (2019) 58.
- [27] G. L. Kane, C. F. Kolda, L. Roszkowski and J. D. Wells, Phys. Rev. D **49** (1994) 6173.

- [28] H. Baer, C. H. Chen, R. B. Munroe, F. E. Paige and X. Tata, Phys. Rev. D **51** (1995) 1046.
- [29] R. Barbieri and G. F. Giudice, Nucl. Phys. B **306**, 63 (1988).
- [30] G. W. Anderson and D. J. Castano, Phys. Rev. D **53** (1996) 2403.
- [31] K. L. Chan, U. Chattopadhyay and P. Nath, Phys. Rev. D **58**, 096004 (1998); J. L. Feng, K. T. Matchev and T. Moroi, Phys. Rev. Lett. **84** (2000) 2322; J. L. Feng, K. T. Matchev and T. Moroi, Phys. Rev. D **61** (2000) 075005.
- [32] H. Baer, V. Barger and A. Mustafayev, JHEP **1205** (2012) 091.
- [33] H. Baer, V. Barger, D. Mickelson and M. Padeffke-Kirkland, Phys. Rev. D **89** (2014) no.11, 115019.
- [34] D. Matalliotakis and H. P. Nilles, Nucl. Phys. B **435** (1995) 115; M. Olechowski and S. Pokorski, Phys. Lett. B **344** (1995) 201; P. Nath and R. L. Arnowitt, Phys. Rev. D **56** (1997) 2820; J. Ellis, K. Olive and Y. Santoso, Phys. Lett. **B539** (2002) 107; J. Ellis, T. Falk, K. Olive and Y. Santoso, Nucl. Phys. **B652** (2003) 259; H. Baer, A. Mustafayev, S. Profumo, A. Belyaev and X. Tata, JHEP**0507** (2005) 065.
- [35] F. E. Paige, S. D. Protopopescu, H. Baer and X. Tata, hep-ph/0312045.
- [36] H. Baer, V. Barger, J. S. Gainer, H. Serce and X. Tata, Phys. Rev. D **96** (2017) no.11, 115008.
- [37] H. Baer, V. Barger, J. S. Gainer, D. Sengupta, H. Serce and X. Tata, Phys. Rev. D **98** (2018) no.7, 075010.
- [38] H. P. Nilles and P. K. S. Vaudrevange, Adv. Ser. Direct. High Energy Phys. **22** (2015) 49.
- [39] W. Buchmuller, K. Hamaguchi, O. Lebedev and M. Ratz, hep-ph/0512326.
- [40] The ATLAS collaboration [ATLAS Collaboration], ATLAS-CONF-2018-041.
- [41] A. M. Sirunyan *et al.* [CMS Collaboration], JHEP **1710**, 019 (2017) doi:10.1007/JHEP10(2017)019 [arXiv:1706.04402 [hep-ex]].
- [42] A. M. Sirunyan *et al.* [CMS Collaboration], JHEP **1809**, 007 (2018) doi:10.1007/JHEP09(2018)007 [arXiv:1803.06553 [hep-ex]].
- [43] M. Aaboud *et al.* [ATLAS Collaboration], Phys. Rev. D **97**, no. 5, 052010 (2018) doi:10.1103/PhysRevD.97.052010 [arXiv:1712.08119 [hep-ex]].
- [44] E. Aprile *et al.* [XENON Collaboration], Phys. Rev. Lett. **121** (2018) no.11, 111302.
- [45] H. Baer, V. Barger, J. S. Gainer, P. Huang, M. Savoy, D. Sengupta and X. Tata, Eur. Phys. J. C **77** (2017) no.7, 499.

- [46] H. Baer, V. Barger, M. Padeffke-Kirkland and X. Tata, Phys. Rev. D **89** (2014) no.3, 037701.
- [47] H. Baer, V. Barger, P. Huang, D. Mickelson, A. Mustafayev, W. Sreethawong and X. Tata, Phys. Rev. Lett. **110** (2013) no.15, 151801.
- [48] H. Baer, V. Barger, P. Huang, D. Mickelson, A. Mustafayev, W. Sreethawong and X. Tata, JHEP **1312** (2013) 013 Erratum: [JHEP **1506** (2015) 053].
- [49] H. Baer, V. Barger, J. S. Gainer, M. Savoy, D. Sengupta and X. Tata, Phys. Rev. D **97** (2018) no.3, 035012.
- [50] Z. Han, G. D. Kribs, A. Martin and A. Menon, Phys. Rev. D **89** (2014) no.7, 075007; H. Baer, A. Mustafayev and X. Tata, Phys. Rev. D **90** (2014) no.11, 115007; C. Han, D. Kim, S. Munir and M. Park, JHEP **1504** (2015) 132.
- [51] A. M. Sirunyan *et al.* [CMS Collaboration], Phys. Lett. B **782** (2018) 440.
- [52] X. Cid Vidal *et al.*, arXiv:1812.07831 [hep-ph].
- [53] H. Baer, M. Bisset, C. Kao and X. Tata, Phys. Rev. D **50** (1994) 316.
- [54] K. J. Bae, H. Baer, N. Nagata and H. Serce, Phys. Rev. D **92** (2015) no.3, 035006.
- [55] H. Baer, V. Barger and P. Huang, JHEP **1111** (2011) 031.
- [56] R. Allahverdi, B. Dutta and K. Sinha, Phys. Rev. D **86**, 095016 (2012).
- [57] H. Baer, V. Barger and D. Mickelson, Phys. Lett. B **726** (2013) 330.
- [58] K. J. Bae, H. Baer, V. Barger, D. Sengupta, to appear.
- [59] H. Baer, V. Barger, D. Sengupta and X. Tata, Eur. Phys. J. C **78** (2018) no.10, 838
- [60] K. J. Bae, H. Baer, A. Lessa and H. Serce, JCAP **1410** (2014) no.10, 082.
- [61] E. Aprile *et al.* [XENON100 Collaboration], arXiv:1609.06154 [astro-ph.CO].
- [62] D. S. Akerib *et al.* [LUX-ZEPLIN Collaboration], arXiv:1802.06039 [astro-ph.IM].
- [63] see talks given at UCLA DM 2018 by Giuliana Fiorillo and by Cristiano Galbiati for the future DarkSide-20k and GADMC detector reaches.
- [64] C. Amole *et al.* [PICO Collaboration], Phys. Rev. Lett. **118** (2017) no.25, 251301.
- [65] M. G. Aartsen *et al.* [IceCube Collaboration], Eur. Phys. J. C **77** (2017) no.3, 146.
- [66] M. L. Ahnen *et al.* [MAGIC and Fermi-LAT Collaborations], JCAP **1602**, no. 02, 039 (2016) doi:10.1088/1475-7516/2016/02/039 [arXiv:1601.06590 [astro-ph.HE]].
- [67] K. J. Bae, H. Baer and H. Serce, JCAP **1706** (2017) no.06, 024.